



Cellulose-stabilized oil-in-water emulsions: Structural features, microrheology, and stability

Carolina Costa^{a,*}, Pedro Rosa^b, Alexandra Filipe^c, Bruno Medronho^{a,b}, Anabela Romano^b, Lucy Liberman^{d,1}, Yeshayahu Talmon^d, Magnus Norgren^a

^a FSCN, Surface and Colloid Engineering, Mid Sweden University, SE-85170 Sundsvall, Sweden

^b MED – Mediterranean Institute for Agriculture, Environment and Development, University of Algarve, Faculty of Sciences and Technology, Campus de Gambelas, Ed. 8, 8005-139 Faro, Portugal

^c CIEPQPF, Department of Chemical Engineering, University of Coimbra, Pólo II – R. Silvío Lima, 3030-790 Coimbra, Portugal

^d Department of Chemical Engineering and the Russell Berrie Nanotechnology Institute (RBNI), Technion-Israel Institute of Technology, Haifa 3200003, Israel

ARTICLE INFO

Keywords:

Cellulose
Emulsions
Microrheology
Diffusing wave spectroscopy
Cryo-scanning electron microscopy

ABSTRACT

Cellulose-based oil-in-water (O/W) emulsions were studied by diffusing wave spectroscopy (DWS) regarding the effect of the cellulose concentration and mixing rate on the average droplet size, microrheological features and stability. Furthermore, the microstructure of these emulsions was imaged by cryo-scanning electron microscopy (cryo-SEM). The micrographs showed that cellulose was effectively adsorbed at the oil-water interface, resembling a film-like shell that protected the oil droplets from coalescing. The non-adsorbed cellulose that was observed in the continuous aqueous medium, contributed to the enhancement of the viscosity of the medium, leading to an improvement in the stability of the overall system. Generally, the higher the cellulose concentration and mixing rate, the smaller the emulsion droplets formed, and the higher was their stability. The combination of both techniques, DWS and cryo-SEM, revealed a very appealing and robust methodology for the characterization and design of novel emulsion-based formulations.

1. Introduction

Emulsions can be simplistically defined as dispersions of an immiscible liquid into another (Tadros, 2013). The dispersed phase is formed by droplets that are surrounded by a fluid referred to as the continuous phase. Emulsions can be categorized as oil-in-water (O/W) or water-in-oil (W/O), depending on the liquids that form the continuous and dispersed phases. Depending on the final application, a variety of emulsifying and stabilizing agents can be selected, such as surfactants, polymers or solid particles, which are meant to adsorb at the O/W interface (Salager, Forgiarini, & Bullón, 2014). The number of applications where emulsions take part is quite vast, embracing different areas as, for instance, food and health sectors, as well as chemical synthesis (Förster & Rybinski, 1998; Hougeir & Kircik, 2012; McClements, 2016; Salager, Moreno, Antón, & Marfisi, 2002). The tuning of the physical properties of the emulsions, such as droplet size, flow behaviour and physical stability, are important to obtain a final product with superior

characteristics (McClements & Gumus, 2016; Tadros, 2013). Moreover, the knowledge of the flow properties of an emulsion is of major importance for the optimal design and scale-up in the manufacturing processes (e.g., mixing, pumping, pouring, extruding, draining, etc.) and storage (e.g., shelf life and temperature) of the end product (Barnes, 1994; Tadros, 2004). Therefore, the study of the emulsions rheological behaviour is quite relevant, due to its intrinsic sensitivity to the oil and aqueous volume fractions, the size of droplets, and the physical features of the emulsifying agent (Corredig & Alexander, 2008; Tadros, 2013).

Since emulsions are thermodynamically unstable, emulsifiers and stabilizers are required to enhance their long-term stability. They may add electrostatic and steric repulsions, or a mechanical barrier (particle stabilization). In many cases, more than one mechanism is present at the same time (Holmberg, Jönsson, Kronberg, & Lindman, 2002). The majority of the emulsifiers used nowadays in the industry still have a synthetic or animal-based origin (McClements & Gumus, 2016). In the last two decades, research has been much dedicated to find plant-based

* Corresponding author.

E-mail addresses: carolina.costa@miun.se (C. Costa), a57578@ualg.pt (P. Rosa), alexandraf@eq.uc.pt (A. Filipe), bmedronho@ualg.pt (B. Medronho), aromano@ualg.pt (A. Romano), lucylib@technion.ac.il (L. Liberman), ishi@technion.ac.il (Y. Talmon), magnus.norgren@miun.se (M. Norgren).

¹ Present address: Departments of Chemistry of Chemical Engineering & Materials Science, University of Minnesota, Minneapolis, MN 55455, USA.

<https://doi.org/10.1016/j.carbpol.2020.117092>

Received 21 February 2020; Received in revised form 13 August 2020; Accepted 11 September 2020

Available online 15 September 2020

0144-8617/© 2020 The Authors. Published by Elsevier Ltd. This is an open access article under the CC BY license (<http://creativecommons.org/licenses/by/4.0/>).

alternatives, primarily focusing on their biocompatibility and low toxicity (Bouyer, Mekhloufi, Rosilio, Grossiord, & Agnely, 2012; McClements & Gumus, 2016). Among the candidates, cellulose has emerged as a very promising emulsifying agent (Costa, Medronho et al., 2019). It is an economically viable biomaterial for various industrial applications, since it is the most abundant, biodegradable, and renewable biopolymer on earth (Klemm, Philipp, Heinze, Heinze, & Wagenknecht, 1998). It can be sourced from plants, biomass, or bacteria with efficiently scalable isolation techniques (Bajpai, 2018; Radotić & Mičić, 2016; Szymańska-Chargot, Chylińska, Gdula, Koziol, & Zdunek, 2017). More importantly, cellulose is an amphiphilic biopolymer and all its forms, from polymeric to nanocrystals and fibrils, can produce fairly stable emulsions, providing quite a versatile natural source of stabilizers (Costa, Medronho et al., 2019). Around the droplets, cellulose creates a powerful mechanical barrier against coalescence and lipid oxidation, contributing to superior stabilization (Kargar, Fayazmanesh, Alavi, Spyropoulos, & Norton, 2012; Oza & Frank, 1986, 1989). In addition, non-adsorbed cellulose may be present in the continuous phase, enhancing the viscosity, and forming a 3D interconnected network, which entraps the oil droplets limiting their dynamics and improving the emulsion stability (Jia et al., 2015; Shen, Guo, Wu, Zhang, & Abid, 2016; Winuprasith & Suphantharika, 2015).

The use of polymeric non-derivatized cellulose processed via dissolution and regeneration to stabilize emulsions is a rather recent approach, but the few works available clearly indicate benefits over the use of cellulose nanocrystals and fibrils, particularly regarding the preparation methods and yields (Costa, Medronho et al., 2019). In this respect, we have recently studied the microrheological properties of O/W emulsions stabilized by polymeric cellulose, through DWS (Medronho et al., 2018). Cellulose was dissolved in a phosphoric acid-based solvent and regenerated *in situ* during emulsion formation. It was found that the cellulose hydrolysis time greatly affects the size and stability of the formed emulsions. In the current study, we further explored the influence of cellulose concentration and mixing rate on the emulsions droplet size, microrheology, and stability. Additionally, the microstructural features of two different emulsion systems, one acidic and one alkaline, were accessed by cryo-SEM.

2. Materials and methods

2.1. Emulsions preparation

For the microrheology essays, acidic emulsions containing cellulose and liquid paraffin were prepared. A commercial cellulose pulp from Domsjö Fabriker (Sweden) with a weight-average molecular weight (M_w) of ca. 3.2×10^5 g/mol and a polydispersity index of 10.3, was the cellulose source used as the emulsifying agent. Briefly, solutions of different cellulose concentrations (i.e., 1, 1.5 and 2 wt.%) were initially prepared in an 85 wt.% H_3PO_4 (Sigma Aldrich) aqueous solvent at room temperature, and incubated with agitation for 48 h. The O/W emulsions were then formed by dispersing 10 wt.% (v/v) liquid paraffin (Merck KGaA, Germany) in the different cellulose solutions for 2 min using an Ultra-Turrax mixer at three different speeds (i.e., 16,000, 22,000 and 24,000 rpm). Milli-Q water was added afterwards to induce cellulose regeneration at the O/W interface and the systems were homogenized for 8 min more. The homogenization process was carried at room temperature.

For the cryo-SEM analysis, both acidic and alkaline emulsions were prepared, but with slightly different procedures. In this case, the acidic emulsion containing 1 wt.% cellulose was prepared using ultrasonication instead of high-speed mixing, in order to obtain a narrower size distribution (Costa, Mira et al., 2019). Conversely, the alkaline emulsions were prepared with microcrystalline cellulose (Avicel PH-101 from Sigma Aldrich), due to the limitations of this solvent in dissolving cellulose of higher molecular weight. The alkaline solvent was composed of 8 wt.% NaOH and 6 wt.% thiourea; an Ultra-Turrax

mixer was used to homogenize the system at 24,000 rpm.

2.2. Drop size determination

The median droplet diameter (D_{50}) of the cellulose-based emulsions was determined by laser light scattering using a Mastersizer Hydro 2000SM (Malvern Instruments, UK) instrument. For these measurements, a small volume of the emulsions was added drop-wise into a sample dispersion unit (at 2000 rpm), filled with water, until an optimum measuring value was reached by the program (i.e., an indirect indication of the number of drops).

2.3. Light microscopy

Samples were observed by bright-field light microscopy at 20x magnification, using a Zeiss AxioLabA1 microscope equipped with a camera Zeiss AxioCam 105 color with 5 megapixels. 10 μ l of the emulsions were placed on a glass slide, and covered with a cover-slip; micrographs were recorded and analyzed with the Zen 2.6 software. The average droplet size was determined using the Analyze Particles tool from ImageJ (open source software from the National Institutes of Health, USA). The image threshold and parameters were adjusted to exclude any aggregates from the estimation, ensuring analysis of single droplets only.

2.4. Diffusing wave spectroscopy

A RheoLab instrument (LS Instruments AG, Fribourg, Switzerland), equipped with the echo technology, was used for diffusing wave spectroscopy analysis in the transmission mode. DWS is an advanced light-scattering technique that accesses the microrheology of highly turbid samples by approximating the propagation of light to the diffusion equation and a detailed theoretical framework of this method can be found elsewhere (Niederquell, Völker, & Kuentz, 2012; Reufer et al., 2014). Briefly, an emulsion contains oil droplets that perform Brownian motions, which are sensitive to the rheology of the system. When a laser source illuminates the sample loaded in a cuvette, the photons will be scattered multiple times by the oil droplets. Intensity fluctuations are detected when the scattered photons emerge at the opposite side of the incident light. This intensity fluctuations are then used as a probe to characterize the rheological properties of the sample. A cuvette made of polystyrene, 10 mm in thickness, L, was used and all the samples were vigorously mixed for 10 s, using a vortex mixer, and equilibrated for 900 s in the measuring chamber at 25 °C. The measurement time was set to 240 s with additional 30 s of echo duration. Three individual runs for each sample were performed, and the estimated error was below 5 %.

2.5. Cryo-scanning electron microscopy

Cryo-SEM specimens of the emulsions were prepared by the drop plunging method: A 3 μ L drop of emulsion was applied onto a gold planchette, which was then plunged manually into liquid nitrogen (LN2). The specimens were then loaded into a dedicated Leica 'sample table', and transferred by an LN2-cooled and evacuated Leica VCT-100 shuttle into the Leica BAF060 freeze-fracture system, where the frozen droplets were fractured by a cryogenically cooled knife, exposing the inner part of the drop. The sample table with the fractured specimens were then transferred into the pre-cooled cryo-stage (-145 °C) in the Zeiss Ultra Plus high-resolution SEM, using the evacuated and cooled VCT-100 shuttle. The specimens were not coated, as we worked at low acceleration voltage, at which no specimen charging occurs (Lieberman, Kleinerman, Davidovich, & Talmon, 2020). The specimens were imaged either by an Everhart-Thornley secondary electron detector, or by in-the-column backscattered electron detector. The former gives good topographical contrast of the fractures specimen, while the latter gives good elemental contrast, allowing us to distinguish between the water,

oil, and cellulose (Lieberman et al., 2020).

3. Results

3.1. Electron microscopy of O/W emulsions stabilized by cellulose

Cryo-SEM is a powerful microscopy technique that provides relevant information on the microstructural features of cellulose-stabilized emulsions. In Fig. 1a, a typical cryo-SEM image of emulsions prepared with cellulose dissolved in the acid-based solvent is shown. The emulsion droplets (arrows) have reasonably low polydispersity with a remarkable small average size, most likely due to the ultrasonication applied for homogenization of the system. The arrow in the lower left corner points to two droplets that have partially fused. It seems that droplets were fractured through. Around each we observe the rim of adsorbed cellulose. Arrowheads point to features introduced by the fracturing of the ice matrix.

Conversely, emulsions prepared with cellulose previously dissolved in an alkaline solvent and homogenized with the Ultra-Turrax mixer have an average droplet size considerably larger, as evidenced in Fig. 1b and c. The solvent system determines how much cellulose is available to emulsify the oil fraction and how small are the cellulose entities that rapidly diffuse and adsorb to the newly created O/W interfaces. These differences in the dissolution performance affect, in turn, the size of the emulsion droplets. As shown in our previous work, a decrease in the size of cellulose chains, due to the acidic hydrolysis reaction, leads to a more efficient stabilization of smaller oil droplets (Medronho et al., 2018). Shorter and more flexible fibrils are likely to diffuse faster, and better cover smaller droplets. This is expected to reduce more efficiently the surface tension and stabilize the oil droplets (Costa, Mira et al., 2019; Medronho et al., 2018). However, the alkali solvent has a lower dissolution performance than the acid one.

Remarkably, the droplets observed in the alkaline systems (Fig. 1b and c), also due to their larger size, reveal additional structural features

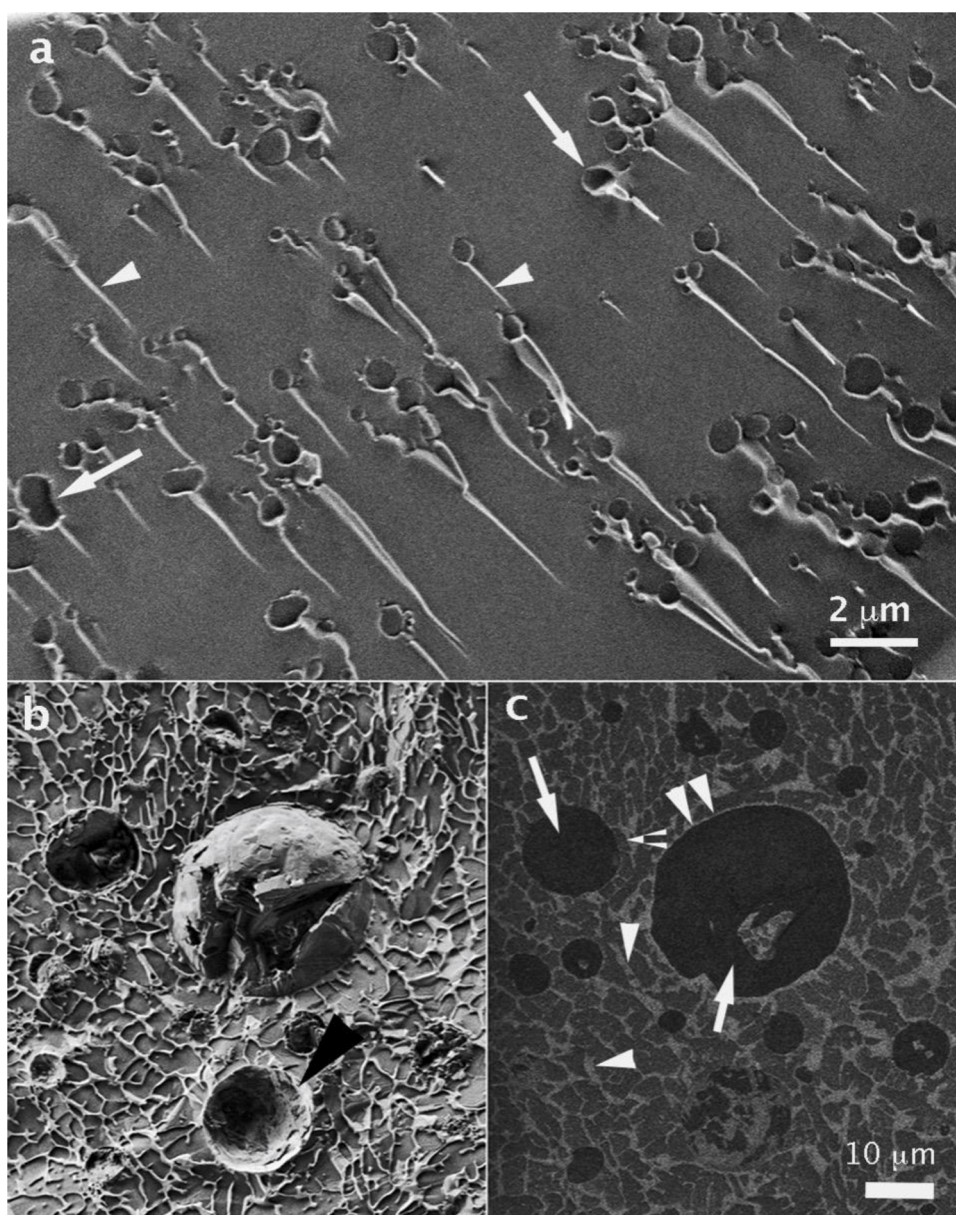


Fig. 1. Representative cryo-SEM images of the emulsions prepared with 1 wt.% cellulose previously dissolved in: (a) 85 wt.% phosphoric acid (secondary electron image); (b) and (c) 8 wt.% NaOH/6 wt.% thiourea (secondary and backscattered electron images, respectively, of the same area). In (c) the darker areas correspond to the oil domains (white arrows), while the water domains are lighter. The brightest areas correspond to cellulose (arrowheads). The black arrowhead in (b) points to the cellulose layer surrounding the oil that had been plucked away by the fracturing of the cryo-specimen.

not fully perceptible in the acidic case. Those are micrographs of the same specimen area taken with the secondary electron detector (Fig. 1b) and with backscattered electron detector (Fig. 1c). Some water was sublimed from the specimen in the cryo-SEM to enhance contrast. Careful observation of Fig. 1b, shows well the topography of the specimen, and unveils the craters left by the oil droplets that were plucked away by the cryo-SEM fracture process, leaving behind an easily visible cellulose coating (black arrow). In Fig. 1c, one sees well the contrast between cellulose (light areas), water (gray areas), and oil (darker areas). This is a most useful feature of performing SEM at low voltage. A cellulose thin layer (double arrowhead) surrounding the oil droplets (white arrows) is also visible. Furthermore, a cellulose network is formed in the continuous phase (arrowheads) by the non-adsorbed cellulose. The so well-structured network may be an artefact induced during specimen freezing, by cellulose being excluded from the forming ice crystals. Overall, the cryo-SEM data suggests that cellulose can stabilize the emulsions via 1) direct adsorption at the O/W interface, thus creating a mechanical barrier between droplets, and 2) by increasing the viscosity of the continuous phase (non-absorbed cellulose) restricting the movement of the oil droplets and their interactions. Despite the use of different solvents, it is believed that the structural features and mechanisms governing emulsion stabilization by cellulose are similar in both systems, since solvents are expected to affect the dynamics of the system during homogenization and consequently the final droplet size, but not the underlying mechanism related to the emulsion stabilization by cellulose. Thus, the data strongly suggests that the dissolution-regeneration protocol of making cellulose-based emulsions will always yield a continuous-like coating at the O/W interface (Costa, Medronho et al., 2019). This has also been evidenced in the related work of Napso et al., where an ionic liquid was used as the cellulose solvent (Napso, Rein, Fu, Radulescu, & Cohen, 2018).

Since cellulose dissolution is more efficient in the acidic aqueous system than in the alkaline solvent, the former has been selected to study the effect of the mixing rate and cellulose concentration on the microrheology and stability of the emulsions formed. The acid system also allows the use of cellulose pulp, thus extending our previous knowledge on cellulose stabilized emulsions (Medronho et al., 2018). The Ultra-Turrax was selected as the mixing apparatus because in large scale productions it is preferred over ultrasonicators.

3.2. Effect of the mixing rate on emulsion droplet size and microrheology

The droplet size depends on the chemistry of the emulsion system and on the energy applied during homogenization. In this context, three different systems were prepared using an Ultra-Turrax at different

mixing rates: 16,000, 22,000 and 24,000 rpm. As it is seen in Fig. 2, the increase in the mixing rate reduces the droplet size, which is more pronounced from 16,000 to 22,000 rpm. Moreover, the droplet size estimated by light microscopy agrees well with the median diameter (D_{50}) obtained by the Mastersizer.

Higher energy input via higher mixing rates promotes better dispersion of the oil in the aqueous phase, leading to the formation of smaller droplets of larger curvature. These results are consistent with our previous work, where the emulsions were prepared with an ultrasonicator (Medronho et al., 2018). In that case, the applied energy during homogenization is higher than that provided by the Ultra-Turrax, and, indeed, smaller emulsion droplets were obtained, ca. $1.76 \pm 0.58 \mu\text{m}$, also in agreement with the cryo-SEM image in the present work (Fig. 1a) (Medronho et al., 2018). In order to evaluate the effect of the droplet size on the microrheology of the emulsions, DWS assays were performed in the transmission mode. The variation of the complex viscosity (η^*) with frequency, for the samples prepared at 16,000, 22,000 and 24,000 rpm, is depicted in Fig. 3a.

A slight increase of the η^* is observed for higher mixing rates. As discussed before, usually, the higher the mixing rate the smaller the emulsion droplets formed. Therefore, the decrease in the droplet size results in a larger number of droplets per unit volume, potentially increasing the contact points and interactions between them, which ultimately increases η^* . In Fig. 3b, the crossover of G' and G'' indicates that the sample is viscoelastic, showing a liquid-like behaviour at low frequencies and a solid-like behaviour at higher frequencies. Similar profiles were obtained for the other two samples prepared at lower mixing rates. Since DWS accesses a more extended frequency range in comparison to the mechanical rheometer, often a second cross-over can be observed at very high frequencies. The short-relaxation time extracted from that second cross-over is most likely due to dissipation mechanisms in the system which may represent conformational rearrangements of the cellulose entities at the O/W interface.

3.3. Effect of the mixing rate on the emulsion stability

DWS determines the emulsions microrheology through the evaluation of the Brownian motion of the particles, which are inferred by the fluctuations in the intensity of the scattered light. The temporal fluctuations of light, $I(t)$, are detected and correlated using a hardware correlator, enabling to obtain the intensity correlation function (ICF) as a decay curve over a lag time (s). Changes in the physical features of the emulsions are expected to affect their dynamics, and, consequently, the ICF or decay curve. Meaning that, low viscosity samples and samples with smaller oil droplets, will have a faster Brownian dynamic and the

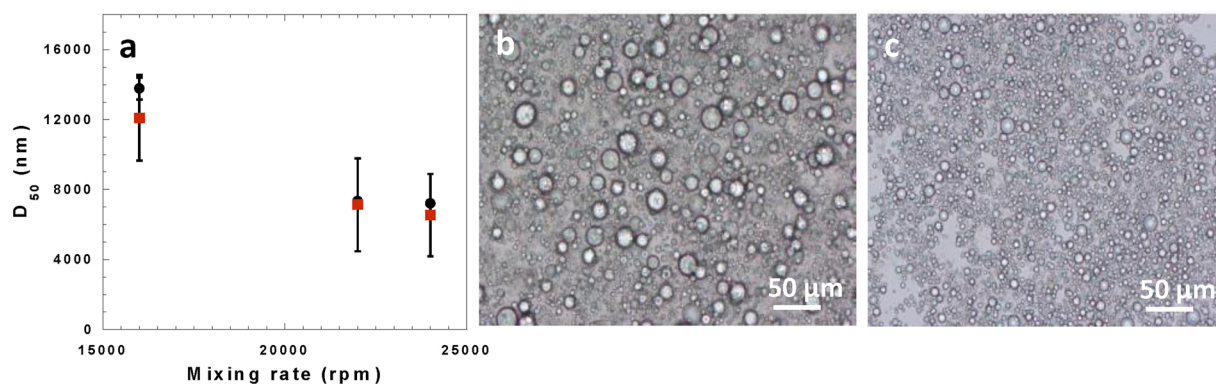


Fig. 2. (a) Median droplet diameter (D_{50}) determined by the Mastersizer (black circles) and by optical microscopy (red squares) as a function of the mixing rate. (b) and (c) Light microscopy images of the emulsions prepared at 16,000 rpm and 24,000 rpm, respectively (For interpretation of the references to colour in this figure legend, the reader is referred to the web version of this article).

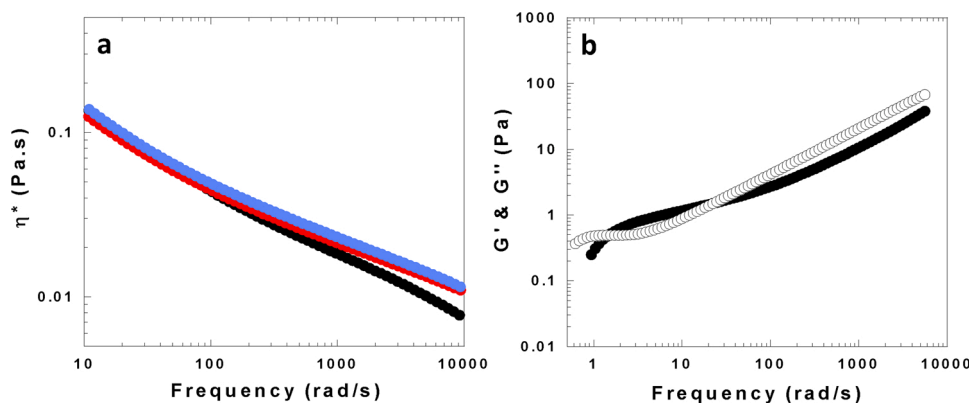


Fig. 3. (a) Complex viscosity, η^* , for samples prepared at 16,000 rpm (black curve), 22,000 rpm (red curve), and 24,000 rpm (blue curve). (b) Viscoelastic parameters, storage modulus (G' , full symbols) and loss modulus (G'' , empty symbols), obtained for the sample prepared at the highest mixing rate (24,000 rpm) (For interpretation of the references to colour in this figure legend, the reader is referred to the web version of this article).

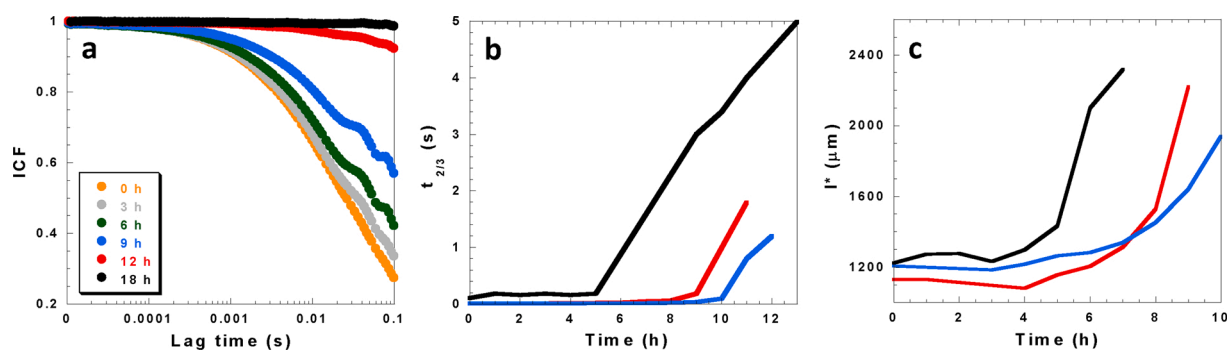


Fig. 4. Stability of the emulsions with ageing: (a) Normalized ICF curves at different ageing times obtained for the system prepared at 24,000 rpm. (b) Decay time ($t_{2/3}$) and (c) transport mean free path (l^*) during the first 12 h of ageing for the systems prepared at 16,000 rpm (black curve), 22,000 rpm (red curve) and 24,000 rpm (blue curve) (For interpretation of the references to colour in this figure legend, the reader is referred to the web version of this article).

ICF decay will occur at shorter lag times. Conversely, the opposite will be verified with an increase in viscosity or droplet's size. This information is of major importance, because it allows the evaluation of the emulsions stability with time. Therefore, measurements were performed every hour for 24 h. Typical ICF curves are shown for the sample prepared at 24,000 rpm (Fig. 4a). A gradual shift towards longer observation times can be observed with ageing, revealing slower dynamics due to the presence of larger particles in solution, most likely from droplet aggregation, which causes the emulsions to cream (Costa, Mira et al., 2019). When the lower detection limit of the equipment is reached, due to the almost complete movement arrest of the oil droplets in the continuous phase, the ICF curve reaches a plateau, which indicates the complete phase separation of the system. The time when the physical destabilization of the oil droplets starts, can be estimated by the $t_{2/3}$ parameter that corresponds to the time at which the normalized ICF decays to 2/3 of its initial value. This parameter was determined for all emulsions with the different mixing rates and plotted against the ageing times (Fig. 4b). The $t_{2/3}$ parameter is approximately zero during the first hours of ageing, indicating the time frame where the Brownian motions of the particles are not significantly altered (i.e., the decay of the ICF curves occurs at the same lag time). After some hours, the $t_{2/3}$ parameter drastically increases as a result of the slowdown of the oil droplets due to their physical destabilization/size increase. This alteration in the $t_{2/3}$ parameter is progressively delayed for emulsions prepared at higher mixing rates; the smaller the oil droplets the more stable the emulsions

become.

The transport mean free path, l^* , was also assessed, and can be described as the average distance a photon needs to travel in the sample before its direction of propagation is randomized. This parameter refers to the optical properties of the sample, and it is highly dependent on the size of the scatterers. If the rheological properties of the continuous phase are not altered with ageing, l^* can be directly correlated with the size of the scatterers and used to evaluate the stability of the emulsions. This is verified because, at a constant volume fraction, the increase in droplet's size, as a consequence of thermodynamic instability, will result in less droplets in the solution and less scattering. Consequently, the photons will need to travel further until their direction is completely randomized and hence l^* will increase. The evolution of l^* with ageing was found to follow the same trend as $t_{2/3}$ (Fig. 4c). These results are in accordance with the ones previously obtained for the emulsions prepared using ultrasonication (Medronho et al., 2018). The present data further suggest that DWS gives powerful microrheological analysis, thus it is a reliable and quite sensitive tool to evaluate the stability of emulsions.

3.4. Influence of cellulose concentration on the emulsion droplet size and microrheology

To evaluate the effect of the cellulose concentration on the emulsions physical features, samples with 1 wt.%, 1.5 wt.% and 2 wt.% cellulose

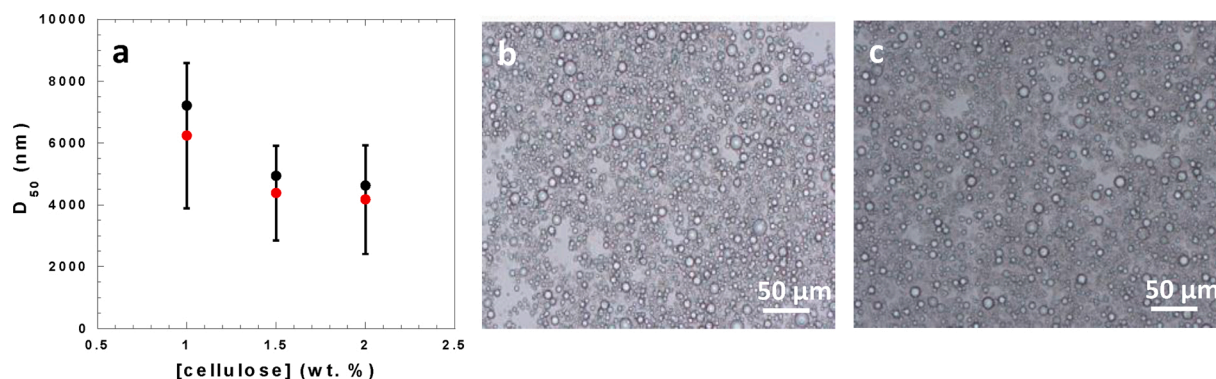


Fig. 5. (a) Median droplet diameter (D_{50}) determined by the Mastersizer (black circles) and by light microscopy (red circles) as a function of cellulose concentration. (b) and (c) Light microscopy images of the emulsions prepared with 1 and 2 wt.% cellulose, respectively (For interpretation of the references to colour in this figure legend, the reader is referred to the web version of this article).

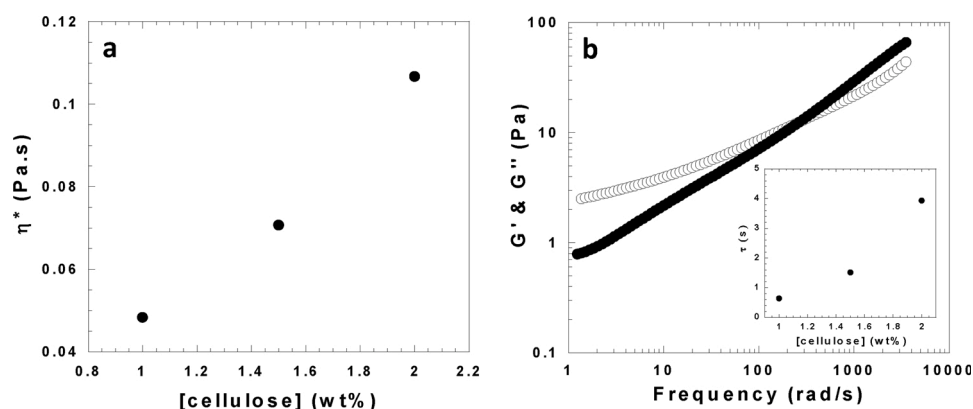


Fig. 6. (a) Complex viscosity, η^* , as a function of cellulose concentration and (b) viscoelastic parameters, storage modulus (G' , full symbols) and loss modulus (G'' , empty symbols), obtained for the 2 wt.% sample. The insert represents the main relaxation time as a function of cellulose concentration.

were also prepared at a mixing rate of 24,000 rpm. The highest mixing rate was selected due to the higher stability with ageing attained for the formed emulsions. The size of the oil droplets was determined, and the optical microrheology was evaluated through DWS assays. Fig. 5 shows the effect of the cellulose concentration on the size of the emulsion droplets.

The results show that the average size of the emulsions decreases with cellulose concentration. As observed in the cryo-SEM images, cellulose adsorbs preferentially at the O/W interface. Therefore, if a more

cellulose is available during homogenization, the surface of the recently formed oil droplets will be more efficiently covered resulting in the overall reduction of the emulsion size and, consequently, in better stabilization. Apparently, above 1.5 wt.% cellulose, additional cellulose in solution has no major effect on the droplet size. It is suggested that the oil droplet surfaces are saturated with cellulose entities, and thus further addition of cellulose does not affect the cellulose adsorbed at the O/W interface, but leads to considerably increase of the viscosity of the emulsions. In Fig. 6a, η^* is plotted as a function of the cellulose

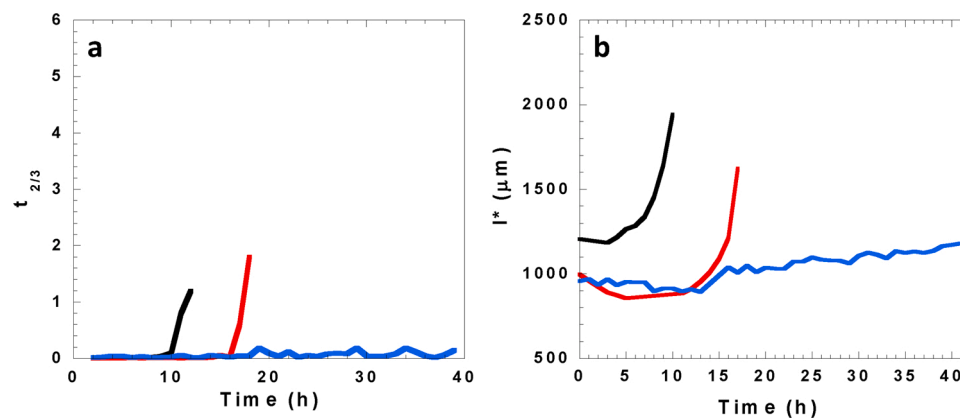


Fig. 7. Evolution of the (a) $t_{2/3}$ and (b) l^* parameters during the first 48 h of ageing for emulsions containing 1 wt.% (black), 1.5 wt.% (red) and 2 wt.% (blue) cellulose (For interpretation of the references to colour in this figure legend, the reader is referred to the web version of this article).

concentration.

As discussed before, the smaller the emulsion droplets formed, the higher the number of droplets per unit of volume, and the increased number of contact points and interactions between them results in the increase of the complex viscosity. Moreover, the excess of non-adsorbed cellulose present in the continuous phase, also shown by cryo-SEM, may also contribute to enhance the overall viscosity of the system. In fact, the main relaxation time (insert in Fig. 6b) increases with cellulose concentration. The longer relaxations obtained for higher cellulose concentrations suggest that the system dynamics become progressively hindered, and therefore better stability with ageing may be anticipated. This hypothesis has been tested with the DWS measurements, where the ICF decay curves and the correspondent $t_{2/3}$ and L^* parameters were evaluated as a function of the cellulose concentration (Fig. 7).

We observe that the sample containing 1.5 wt.% cellulose was stable (against creaming) for approximately 15 h. Remarkably, the sample containing 2 wt.% cellulose was stable for at least 48 h, the duration time of the assay. This superior stability of the emulsions for higher cellulose concentrations is believed to be due to the efficient cover of the O/W interface of the droplets combined with the viscosity enhancement of the continuous phase, which restricts the droplet dynamics, thus minimizing the effect of the major destabilization mechanisms.

4. Conclusions

Cellulose-stabilized O/W emulsions were studied by DWS regarding the effect of the mixing rate and cellulose concentration on the emulsion average droplet size, microrheological properties and stability. It was observed that the smaller the emulsion droplets produced by higher mixing rates, the more stable the system was. Also, the emulsions stability was further improved by higher cellulose concentrations. It is suggested that, a more efficient interfacial coverage of the droplets combined with an enhanced viscosity of the aqueous continuous phase, results in a more stable emulsion. The structural features imaged by cryo-SEM support this conclusion, as cellulose is observed to be adsorbed at the interface of the droplets and dispersed in the continuous aqueous medium. Moreover, cryo-SEM allowed to perceive the shape of the cellulose coating which resembled a film-like shell protecting the oil droplets from coalescing. A hypothesis we previously stated for the shape of the cellulose coatings created through the dissolution-regeneration protocol of making cellulose-based emulsions.

DWS and cryo-SEM combined, revealed a very appealing and robust methodology for the characterization and design of novel emulsion-based formulations. DWS proved to be a very powerful technique to follow subtle changes in the microrheology of emulsions that are not accessed by conventional mechanical rheometry. Moreover, it allows the monitoring of real-time changes in the stability of the emulsions, which is of major importance for the design and optimization of emulsion-based formulations, an efficient production and storage control.

CRediT authorship contribution statement

Carolina Costa: Conceptualization, Supervision, Writing - original draft. **Pedro Rosa:** Investigation, Visualization. **Alexandra Filipe:** Methodology, Data curation, Writing - original draft. **Bruno Medronho:** Funding acquisition, Writing - review & editing. **Anabela Romano:** Writing - review & editing. **Lucy Liberman:** Investigation. **Yeshayahu Talmon:** Writing - review & editing. **Magnus Norgren:** Supervision, Funding acquisition, Writing - review & editing.

Declaration of Competing Interest

The authors report no declarations of interest.

Acknowledgments

This research was funded by the Swedish Research Council (Vetenskapsrådet), grant number 2015-04290. Bruno Medronho acknowledges the financial support from the Portuguese Foundation for Science and Technology, FCT, via the projects PTDC/ASP-SIL/30619/2017, UIDB/05183/2020 and the researcher grant CEECIND/01014/2018. The cryo-SEM work was performed in the Technion Center for Electron Microscopy of Soft Matter, supported by the Technion Russell Berrie Nanotechnology Institute (RBNI).

References

- Bajpai, P. (2018). Chapter 12 - Pulp fundamentals. In P. Bajpai (Ed.), *Biermann's handbook of pulp and paper* (third edition, pp. 295–351). Elsevier.
- Barnes, H. A. (1994). Rheology of emulsions - a review. *Colloids and Surfaces A: Physicochemical and Engineering Aspects*, 91, 89–95. [https://doi.org/10.1016/0927-7757\(93\)02719-U](https://doi.org/10.1016/0927-7757(93)02719-U)
- Bouyer, E., Mekhloufi, G., Rosilio, V., Grossiord, J.-L., & Agnely, F. (2012). Proteins, polysaccharides, and their complexes used as stabilizers for emulsions: Alternatives to synthetic surfactants in the pharmaceutical field? *International Journal of Pharmaceutics*, 436(1–2), 359–378. <https://doi.org/10.1016/j.ijpharm.2012.06.052>
- Corredig, M., & Alexander, M. (2008). Food emulsions studied by DWS: Recent advances. *Trends in Food Science & Technology*, 19(2), 67–75. <https://doi.org/10.1016/j.tifs.2007.07.014>
- Costa, C., Medronho, B., Filipe, A., Mira, I., Lindman, B., Edlund, H., et al. (2019). Emulsion formation and stabilization by biomolecules: The leading role of cellulose. *Polymers*, 11(10). <https://doi.org/10.3390/polym11101570>
- Costa, C., Mira, I., Benjamins, J.-W., Lindman, B., Edlund, H., & Norgren, M. (2019). Interfacial activity and emulsion stabilization of dissolved cellulose. *Journal of Molecular Liquids*. <https://doi.org/10.1016/j.molliq.2019.111325>, 111325.
- Förster, T., & Rybinski, W. v. (1998). Applications of emulsions. *Modern aspects of emulsion science* (pp. 395–426). The Royal Society of Chemistry.
- Holmberg, K., Jönsson, B., Kronberg, B., & Lindman, B. (2002). Emulsions and emulsifiers. *Surfactants and polymers in aqueous solution* (pp. 451–471). John Wiley & Sons, Ltd..
- Hougeir, F. G., & Kircik, L. (2012). A review of delivery systems in cosmetics. *Dermatologic Therapy*, 25(3), 234–237. <https://doi.org/10.1111/j.1529-8019.2012.01501.x>
- Jia, X., Xu, R., Shen, W., Xie, M., Abid, M., Jabbar, S., & Wu, T. (2015). Stabilizing oil-in-water emulsion with amorphous cellulose. *Food Hydrocolloids*, 43, 275–282. <https://doi.org/10.1016/j.foodhyd.2014.05.024>
- Kargar, M., Fayazmanesh, K., Alavi, M., Spyropoulos, F., & Norton, I. T. (2012). Investigation into the potential ability of Pickering emulsions (food-grade particles) to enhance the oxidative stability of oil-in-water emulsions. *Journal of Colloid and Interface Science*, 366(1), 209–215. <https://doi.org/10.1016/j.jcis.2011.09.073>
- Klemm, D., Philipp, B., Heinze, T., Heinze, U., & Wagenknecht, W. (1998). Introduction. *Comprehensive cellulose chemistry* (pp. 1–7). Wiley-VCH Verlag GmbH & Co. KGaA.
- Liberman, L., Kleinerman, O., Davidovich, I., & Talmon, Y. (2020). Micrograph contrast in low-voltage SEM and cryo-SEM. *Ultramicroscopy* (under review).
- McClements, D. J. (2016). *Food emulsions: Principles, practices and techniques* (3rd edition ed.). Boca Raton: CRC Press.
- McClements, D. J., & Gumus, C. E. (2016). Natural emulsifiers - Biosurfactants, phospholipids, biopolymers, and colloidal particles: Molecular and physicochemical basis of functional performance. *Advances in Colloid and Interface Science*, 234, 3–26. <https://doi.org/10.1016/j.cis.2016.03.002>
- Medronho, B., Filipe, A., Costa, C., Romano, A., Lindman, B., Edlund, H., et al. (2018). Microrheology of novel cellulose stabilized oil-in-water emulsions. *Journal of Colloid and Interface Science*, 531, 225–232. <https://doi.org/10.1016/j.jcis.2018.07.043>
- Napso, S., Rein, D. M., Fu, Z., Radulescu, A., & Cohen, Y. (2018). Structural analysis of cellulose-coated oil-in-water emulsions fabricated from molecular solution. *Langmuir*, 34(30), 8857–8865. <https://doi.org/10.1021/acs.langmuir.8b01325>
- Niederquell, A., Völker, A. C., & Kuentz, M. (2012). Introduction of diffusing wave spectroscopy to study self-emulsifying drug delivery systems with respect to liquid filling of capsules. *International Journal of Pharmaceutics*, 426(1), 144–152. <https://doi.org/10.1016/j.ijpharm.2012.01.042>
- Oza, K. P., & Frank, S. G. (1986). Microcrystalline cellulose stabilized emulsions. *Journal of Dispersion Science and Technology*, 7(5), 543–561. <https://doi.org/10.1080/01932698608943478>
- Oza, K. P., & Frank, S. G. (1989). Multiple emulsions stabilized by colloidal microcrystalline cellulose. *Journal of Dispersion Science and Technology*, 10(2), 163–185. <https://doi.org/10.1080/01932698908943168>
- Radotić, K., & Micić, M. (2016). Methods for extraction and purification of lignin and cellulose from plant tissues. In M. Micić (Ed.), *Sample preparation techniques for soil, plant, and animal samples* (pp. 365–376). New York, NY: Springer New York.
- Reufer, M., Machado, A. H. E., Niederquell, A., Bohnenblust, K., Müller, B., Völker, A. C., et al. (2014). Introducing diffusing wave spectroscopy as a process analytical tool for pharmaceutical emulsion manufacturing. *Journal of Pharmaceutical Sciences*, 103(12), 3902–3913. <https://doi.org/10.1002/jps.24197>
- Salager, J.-L., Forgiarini, A., & Bullón, J. (2014). Progress in designing emulsion properties over a century: Emerging phenomenological guidelines from generalized formulation and prospects to transmute the knowledge into know-how. In

- L. S. Romsted (Ed.), *Surfactant science and technology: Retrospects and prospects* (1st edition ed., pp. 459–487). Boca Raton: CRC Press.
- Salager, J.-L., Moreno, N., Antón, R., & Marfisi, S. (2002). Apparent equilibration time required for a surfactant–oil–water system to emulsify into the morphology imposed by the formulation. *Langmuir*, 18(3), 607–611. <https://doi.org/10.1021/la010582d>
- Shen, W., Guo, L., Wu, T., Zhang, W. H., & Abid, M. (2016). Stabilizing beverage emulsions by regenerated celluloses. *LWT-Food Science and Technology*, 72, 292–301. <https://doi.org/10.1016/j.lwt.2016.05.012>
- Szymańska-Chargot, M., Chylińska, M., Gdula, K., Koziol, A., & Zdunek, A. (2017). Isolation and characterization of cellulose from different fruit and vegetable pomaces. *Polymers*, 9(10). <https://doi.org/10.3390/polym9100495>
- Tadros, T. (2004). Application of rheology for assessment and prediction of the long-term physical stability of emulsions. *Advances in Colloid and Interface Science*, 108–109, 227–258. <https://doi.org/10.1016/j.cis.2003.10.025>
- Tadros, T. (2013). Emulsion formation, stability, and rheology. *Emulsion Formation and Stability*, 1–75. <https://doi.org/10.1002/9783527647941.ch1>
- Winuprasith, T., & Suphantharika, M. (2015). Properties and stability of oil-in-water emulsions stabilized by microfibrillated cellulose from mangosteen rind. *Food Hydrocolloids*, 43, 690–699. <https://doi.org/10.1016/j.foodhyd.2014.07.027>